Title

Using seconds-resolved pharmacokinetic datasets to assess pharmacokinetic models encompassing time-varying physiology.

Journal

British Journal of Clinical Pharmacology, 89(9)

Authors

McDonough, Matthew

Stocker, Sophie

Kippin, Tod

et al.

Publication Date

2023-09-01

DOI

10.1111/bcp.15756

Peer reviewed

HHS Public Access

Author manuscript

Br J Clin Pharmacol. Author manuscript; available in PMC 2024 September 01.

Published in final edited form as:

Br J Clin Pharmacol. 2023 September ; 89(9): 2798–2812. doi:10.1111/bcp.15756.

Using seconds-resolved pharmacokinetic datasets to assess pharmacokinetic models encompassing time-varying physiology

Matthew H. McDonough[a], **Sophie L. Stocker**[b,c], **Tod Kippin**[d,e], **Wendy Meiring**[a,*], **Kevin W. Plaxco**[f,g,*]

[a]Department of Statistics and Applied Probability, University of California Santa Barbara, Santa Barbara, CA 93106, USA.

[b]School of Pharmacy, Faculty of Medicine and Health, University of Sydney, Camperdown NSW 2006, Sydney, Australia.

[c]St Vincent's Clinical School, University of New South Wales, Sydney, Australia.

[d]Department of Psychological and Brain Sciences, University of California Santa Barbara, Santa Barbara, CA 93106, USA.

[e]The Neuroscience Research Institute and Department of Molecular Cellular and Developmental Biology, University of California Santa Barbara, Santa Barbara, CA 93106, USA.

[f]Department of Chemistry and Biochemistry, University of California Santa Barbara, Santa Barbara, CA 93106, USA.

[g]Center for Bioengineering, University of California Santa Barbara, Santa Barbara, CA 93106, USA.

Abstract

Aim—Pharmacokinetics have historically been assessed using drug concentration data obtained via blood draws and bench-top analysis. The cumbersome nature of these typically constrains studies to at most a dozen concentration measurements per dosing event. This, in turn, limits our statistical power in the detection of hours-scale, time-varying physiological processes. Given recent advent of *in-vivo* electrochemical aptamer-based (EAB) sensors, however, we can now obtain hundreds of concentration measurements per administration. Our aim in this paper is to assess the ability of these time-dense datasets to describe time-varying pharmacokinetic models with good statistical significance.

[*]Corresponding authors. meiring@ucsb.edu and kwp@ucsb.edu.

Author Contributions

Major draft writing was done by Matthew H. McDonough, Wendy Meiring, and Kevin W. Plaxco. Statistical Analysis, data visualization, and analysis code was conducted by Matthew H. McDonough. Critical input and insight was provided by Tod Kippin and Sophie L. Stocker. All authors participated in reviewing and editing of this manuscript.

Conflict of interest disclosure

KWP serves on the advisory board and holds equity in a company that is commercializing EAB sensors.

Supporting information

Additional supporting information can be found in the online version of this article on the publisher's website.

Nomenclature of Targets and Ligands

Key protein targets and ligands in this article are hyperlinked to corresponding entries in http://www.guidetopharmacology.org.

Methods—Here we use seconds-resolved measurements of plasma tobramycin concentrations in rats to statistically compare traditional one- and two-compartmental pharmacokinetic models to new models in which the proportional relationship between a drug's plasma concentration and its elimination rate varies in response to changing kidney function.

Results—We find that a modified one-compartment model in which the proportionality between the plasma concentration of tobramycin and its elimination rate falls reciprocally with time either meets or is preferred over the standard two-compartment pharmacokinetic model for half of the datasets characterized. When we reduce the impact of the drug's rapid distribution phase on the model, this one-compartment, time-varying model is statistically preferred over the standard one-compartment model for 80% of our datasets.

Conclusions—Our results highlight both the impact that simple physiological changes (such as varying kidney function) can have on drug pharmacokinetics and the ability of high-time-resolution EAB sensor measurements to identify such impacts.

Keywords

Aminoglycosides; renal function; nonlinear least squares regression; Bayesian Information Criterion; compartment models; animal models

Introduction

Pharmacokinetics, which describe the time-dependent evolution of drug concentrations in blood or other bodily fluids, are typically approximated using simple, compartmental models in which systems of ordinary differential equations (ODEs) represent the rates with which drugs are removed from or transported between one or more (often somewhat abstract) bodily compartments. In a single compartment model, for example, it is assumed that the concentration of the drug is the same throughout the body, rendering the entire subject a single "compartment" from which drug is removed via metabolism or excretion at a rate of which is first-order in (i.e., proportional to) drug concentration. In the next level of model sophistication, the "two-compartment" model, the body is approximated as two compartments which have distinct pharmacokinetic properties. One of these comprises the blood and all rapidly perfused tissues, while the other represents all tissues in which the drug concentration equilibrates more slowly, together leading to pharmacokinetics that are approximated as the sum of two exponential processes. Although simple, these one and two-compartment models are generally adequate to describe the behavior of the drug-concentration time-profile data produced in previous studies. This said, this may only be true because, having relied on cumbersome, labor-intensive blood draws and laboratory analysis for their measurements, these prior studies were typically limited to collecting ten or fewer time points per subject per dosing interval. With so few data points, the ability of such studies to identify other physiological processes affecting pharmacokinetics is likely limited.

As an example of the subtle physiological effects likely missed by prior studies, we note that standard compartmental models employed assume that the rate constants describing the disposition of drugs into and out of the various compartments are, as their name implies, constant over the few-hour time course of the elimination of small molecule drugs. This,

however, is an approximation. For a drug that is excreted via the kidneys, for example, the rate constant for elimination (and thus the drug's half-life; $t_{1/2} = \ln(2)/\text{rate constant}$) depends on kidney function, which varies from hour to hour (e.g., Wang et al., 2010; Arroyo-Currás et al., 2017, 2018b). However, while time-varying pharmacokinetics have been reported over weeks to months timescales have been seen for many drugs (Fontova et al., 2021; Kuypers et al., 2004; Mao et al., 2021; Petitcollin et al., 2020; Wahlby et al., 2004; Wilkins et al., 2019), and changes over days have been seen for the aminoglycosides in ill human patients (Gaskin & Duffull, 1997; Ritchie & Duffull, 1998), we are not aware of any detailed studies of variations occurring over hours. This omission is presumably due to the unduly small number of concentration measurements pharmacokinetic studies have traditionally relied on. Simply put, the time resolution of traditional pharmacokinetic datasets is likely too poor to justify the application of models employing rate parameters that vary over timescales as short as hours at the individual level.

Recently a solution to the problem of limited-density pharmacokinetic datasets has arisen due to advances in *in-vivo* molecular monitoring. Specifically, the development of electrochemical, aptamer-based (EAB) sensors (Xiao et al., 2005) has, for the first time, enabled the collection of seconds-resolved pharmacokinetic datasets comprising hundreds or thousands of drug concentration measurements per dosing interval (Arroyo-Currás et al., 2017, 2018a; Dauphin-Ducharme et al., 2019; Idili et al., 2019; Vieira et al., 2019), with coefficients of variation of better than 10% (Downs et al., 2022) and without detectable time-dependent variations in accuracy (Arroyo-Curras et al., 2017; Leung et al., 2021). And, unlike all prior *in-vivo* molecular measurement approaches, EAB sensors are independent of the chemical (or enzymatic) reactivity of their targets, and thus the technology is a general platform that can be used to measure a wide variety of drug molecules in the body. Motivated by the potential of such time-dense measurements, we have performed a preliminary exploration of what can be done with them using the currently largest dataset of EAB measurements of a drug (Vieira et al., 2019). Specifically, we evaluate pharmacokinetic models employing time-varying elimination rate parameters (i.e., time-varying elimination half-lives) in describing tobramycin plasma concentration profiles in individual rats.

We note that no new animal experiments were conducted in this work. The data used, however, were collected in accordance with animal ethics. Specifically, the housing and care of all rats were conducted in accordance with the guidelines set forth by the "Guide for the Care and Use of Laboratory Animal, 8th edition" (National Research Council (U.S.) et al., 2011) and all experiments were approved by the UCSB Institutional Animal Care and Use Committee.

Results and discussion

As our test case we have employed equally spaced plasma tobramycin concentration measurements collected *in situ* in the jugulars of anesthetized rats with time resolution ranging from 18 to 27 s (Vieira et al., 2019). Prior, *in vivo* studies with the same tobramycin-detecting EAB sensor (Arroyo-Currás et al., 2017) as well as with *in vivo* EAB sensors directed against other drugs (Arroyo-Currás et al., 2017; Chamorro-Garcia et al., 2022; Dauphin-Ducharme et al., 2019) exhibit excellent return to expected, zero drug baselines

after periods in excess of 5 h *in vivo*. Likewise, EAB sensors exhibit good, drift-free operation and retain good measurement accuracy and precision for runs in excess of 24 h when challenged in whole blood *in vitro* at 37°C (e.g., Leung et al., 2021). Together, these reports suggest that the magnitude of any uncorrected EAB sensor drift, which could otherwise mask time-dependent change in pharmacokinetics, is quite small.

The dataset we employed includes plasma concentrations for fourteen individual animals, each dosed with a single, intravenous bolus of tobramycin (20 mg/kg) over a one-minute injection duration. After peak plasma concentrations of tobramycin were observed (presumably denoting the end of the injection), between 63 and 525 concentration measurements were collected on each individual, creating datasets spanning periods of 0.3 to 4 h post-injection. As our study focused on datasets with high time-resolution, we excluded data from four animals reported in Vieira et al. (rats FR5, MR6, MR7, and MR9) that each had less than 1 h of observations after drug administration, and fewer than 167 tobramycin concentrations. The median period of observation in the remaining ten datasets (for four female and six male rats) was 2 h, over which an average of 282 tobramycin concentration measurements were observed per animal. We also excluded data collected more than 2.2 h after administration, as by this time plasma tobramycin concentrations have effectively dropped to zero. Specifically, the plasma half-life of tobramycin in rats is 0.5 h (Reinhard et al., 1994; Wasfi, 1993), and thus, concentrations obtained 2 h after the cessation of drug administration are far below the limit of detection for the EAB sensor employed and are no longer meaningful.

As the basis for the study reported here, we have employed one- and two-compartment pharmacokinetic models with intravenous bolus drug delivery (Loftsson, 2015). In these, the drug is allowed to enter and exit the system of compartments in these models, rendering them “open” models. The one-compartment model treats the entire body as a single compartment (Fig. 1A), termed here the “plasma compartment,” in which the drug is assumed to behave uniformly. In contrast, the two-compartment model (Fig. 1B) separates the body into a first compartment, also termed here the “plasma compartment” (but commonly known as the “central compartment”), that represents the blood plasma and the fluids of any rapidly perfused tissues, and a second, termed the “tissue compartment” (often referred to as the “peripheral compartment”) that represents tissues for which equilibrium is reached more slowly (Loftsson, 2015). In the case of intravenous injection, drugs are assumed to enter the body through the plasma compartment. And drugs that are eliminated unmetabolized via the kidneys, such as tobramycin, also exit the body via this compartment.

In traditional one- and two-compartment models, the rate of change of the plasma concentration at time t includes an elimination component that is proportional to the plasma drug concentration at that time, where the proportionality constant is time-invariant (k_E in subsequent Equations 1 and 3). Here we describe both these traditional models and extensions of the one-compartment model in which the elimination proportionality is time-varying.

The standard one-compartment model describes drug elimination by a first-order, linear ordinary differential equation (ODE) with an initial condition:

$$\frac{dC_P(t)}{dt} = -k_E \cdot C_P(t) \text{ with } C_P(0) = \frac{D_0}{V_P} \quad (1)$$

Here $C_P(t)$ represents the plasma concentration of the drug (in nmol/mL = μmol/L = μM) at time t; k_E represents the rate proportionality constant for the elimination of the drug from the plasma compartment (with units h^{-1}); D_0 is the initial dose of the drug (in nmol). V_P represents the theoretical plasma volume (in mL; this is theoretical because, for example, protein binding reduces the free drug concentration, leading to the theoretical plasma volume being larger than the true plasma volume) (Loftsson, 2015). The negative sign preceding $k_E C_P(t)$ reflects the fact that drug is being removed from the body (for tobramycin this removal is via the kidneys). The solution to Equation 1 is (Aplevich, 2000):

$$C_P(t) = \frac{D_0}{V_0} \cdot \exp\{-k_E \cdot t\} \quad (2)$$

The observed tobramycin plasma concentrations across time are noisy observations of $C_P(t)$. For each dosing event, we estimated the unknown parameters V_P and k_E, in Equation 2 based on these data (D_0 is known).

The standard two-compartment model describes drug elimination by a system of two first-order linear ODEs:

$$\begin{cases} \frac{dC_P(t)}{dt} = k_{DP} \cdot \frac{V_D}{V_P} \cdot C_D(t) - (k_{PD} + k_E) \cdot C_P(t) \\ \frac{dC_D(t)}{dt} = k_{PD} \cdot \frac{V_P}{V_D} \cdot C_P(t) - k_{DP} \cdot C_D(t) \end{cases} \quad (3)$$

with initial conditions $C_P(t) = D_0/V_P$ and $C_D(t) = 0$. Here $C_P(t)$, V_P, k_E, and D_0 are defined as in the standard one-compartment model, $C_D(t)$ represents the drug concentration in the tissue compartment at time t (in μM), V_D the theoretical volume of the tissue compartment, and k_{PD} and k_{DP} the rate constants for drug distribution from the plasma compartment to the tissue compartment and vice versa, respectively (with units h^{-1}). The closed form solution to this model is well-known and is given as (Chen et al., 2014):

$$\begin{cases} C_P(t) = \frac{D_0}{V_P(\alpha - \beta)}\left((\alpha - k_{DP})e^{-\alpha t} + (k_{DP} - \beta)e^{-\beta t}\right) & (4a) \\ C_D(t) = \frac{D_0 \cdot k_{PD}}{V_D(\alpha - \beta)}\left(e^{-\beta t} - e^{-\alpha t}\right) & (4b) \end{cases}$$

where

$$\alpha = \frac{1}{2}\left((k_{PD} + k_{DP} + k_E) + \sqrt{(k_{PD} + k_{DP} + k_E)^2 - 4 \cdot k_{DP} \cdot k_E}\right)$$

$$\beta = \frac{1}{2}\left((k_{PD} + k_{DP} + k_E) - \sqrt{(k_{PD} + k_{DP} + k_E)^2 - 4 \cdot k_{DP} \cdot k_E}\right)$$

Of note, the drug concentration measurements used to constrain two-compartment models almost always are obtained from only the plasma compartment, rendering system (4) incompletely observed. Given this, we estimated four system parameters for each dosing interval considering only the $C_P(t)$ equation in (4); namely V_P, k_E, k_{PD}, and k_{DP}.

To fit the one- and two-compartment models to the observed tobramycin concentrations we used nonlinear least squares regression (Seber & Wild, 2003), and to select between models we used the Bayesian Information Criterion (BIC) (Schwarz, 1978). We used nonlinear least squares regression to estimate the system parameters because $C_P(t)$ is (1) a nonlinear function in each of Equations 2 and 4a, and (2) is subject to measurement error. For model selection, we employed the BIC, which uses the log-likelihood of the candidate model as a goodness-of-fit measure, while simultaneously penalizing model complexity (i.e., in our case, the number of estimated parameters). (Note that the calculation of the log-likelihood here is based on the assumption that the observed concentration measurements equal the true plasma concentration plus random noise perturbations that are independent and normally distributed with a mean of zero and constant variance for each dosing interval.) We chose BIC as our model selection criteria since it increasingly selects the true model (if that model is in the set of candidate models) as the sample size approaches infinity (Warne et al., 2019). Simply put, the candidate model with the lowest BIC is the preferred model, albeit models within two units of the lowest BIC are generally considered to be indistinguishably good descriptions of the system (Fabozzi, 2014). Although here we employ BIC as our primary criterion, for completeness we also report each model's Akaike Information Criterion (AIC) (Akaike, 1974) and in-sample root-mean-square error (RMSE).

Fitting the standard one- and two-compartment models to the observed tobramycin concentrations from a representative female rat (denoted FR1) we find that the one-compartment model (Fig. 2, black curve) fits the concentration-time profile rather poorly at the start and the end of the experiment. In contrast, the standard two-compartment model (Fig. 2, blue curve) fits the data more closely, appropriately capturing an initially rapid decrease in concentration (typically thought to reflect the distribution of the drug from the plasma to the tissues) followed by a slower phase (thought to be elimination of the drug from the body). Consistent with this, the BIC favors (i.e., is lower for) the standard two-compartment model over the one-compartment model for this dataset. I.e., despite the greater complexity of the standard two-compartment model, the smaller BIC it produces indicates that it is preferred over the simpler one-compartment model as a description of these data (shown in Table 2).

We next considered **time-varying one-compartment models** that encompass our hypothesis that the relationship between the drug's plasma concentration and its elimination rate is time-dependent. In these we allow the proportionality factor k_E in Equation 1 to be a function of time t, $k_E(t)$; giving

$$\frac{dC_P(t)}{dt} = -k_E(t) \cdot C_P(t) \quad \text{with} \quad C_P(0) = \frac{D_0}{V_P}. \tag{6}$$

Such models are justified by prior studies indicating that, presumably due to changes in kidney function, the relationship between the plasma concentration and its rate of change varies over the course of just hours in our animal model of tobramycin pharmacokinetics (Arroyo-Currás et al., 2017, 2018b). As the pharmacokinetic data we are exploring were collected on anesthetized animals not on an intravenous drip, we generally expect kidney function and, with this, the proportionality that relates the elimination rate to the drug concentration, to fall monotonically over time (Arroyo-Currás et al., 2017). Given this, we limited our exploration of time-varying one-compartment models to three models in which the proportionality between drug concentration and the elimination rate changes monotonically with time.

The three one-compartment time-varying models we have considered include elimination proportionalities that vary linearly, exponentially, or reciprocally with time. (The three resulting solutions to Equation 6 are shown in Table 1.) We considered the first of these, in which the relationship varies linearly with respect to time, because it is the simplest mathematical extension of the constant proportionality assumed in the standard one-compartment model of Equation 1. In this linear proportionality case, b_E is the rate of change of the elimination term (in h^{-2}), k_{E0} (in h^{-1}) defines the relationship between drug concentration and the elimination rate at time zero. A weakness of this "linearly-varying" one-compartment model is that, under this model, the rate of transport out of the body can become negative, implying the physiologically implausible return of drug to the body from the kidneys. Thus, as two physiologically less naïve time-varying one-compartment models, we allowed the proportionality between drug concentration and elimination rate to fall exponentially or reciprocally over time; we refer to these as the "exponentially-varying one-compartment" and "reciprocally-varying one-compartment" models. In these, b_E (in h^{-1}) controls the rate of change of the proportionality, and k_{E0} (in h^{-1}) defines its value at time zero. If the parameter values in each of these models (b_E and k_{E0}) are positive, we naturally preserve the elimination behavior we desire: the proportionality decreases monotonically while also remaining nonnegative over all time-points. Of note, while these one-compartment time-varying models are more complex than the standard one-compartment model, they are less complex than the standard two-compartment model. Specifically, the time-varying models (Table 1) contain three unknown parameters, V_P, k_{E0}, and b_E, whereas the standard two-compartment model (Equation 4a) contains four.

Fitting our three time-varying one-compartment models to our initial dataset (Fig. 3), we find that all are preferred over both the standard one- and two-compartment models. For

example, these time-varying models also produce substantially lower in-sample root-mean-square errors (RMSEs) than the standard one-compartment model, and similar RMSEs to the standard two-compartment model (Table 2). And while the greater complexity of the time-varying models may render this latter result perhaps unsurprising relative to the standard one-compartment model, the BIC values indicate that the resulting improvements in fit are statistically meaningful. Specifically, the BIC of the exponentially varying model is the smallest by more than two units, thus rendering this the single preferred model to describe the dataset among the five models we have studied.

In all three of our time-varying model fits for FR1, the estimated time-varying elimination proportionalities remained positive over the observation period while nevertheless falling monotonically over time (Fig. 4). Both behaviors match our physiology-based expectations. First, the drug is eliminated via the kidneys and not re-absorbed from them, and thus the proportionality should always remain positive. Second, we expect the elimination proportionality to fall during the experiment as kidney function is reduced by dehydration (the animals were not under an intravenous drip) and reduced blood pressure (due to several hours sedation).

Having used dataset FR1 to hone our thinking, we next fitted all five of our models to the observed concentration-time profiles of the remaining nine animals (Fig. 5; Table 3). From this analysis we draw several conclusions, some expected, others less so. For example, given that prior high-time-resolution studies of tobramycin pharmacokinetics reported good fits to two-compartment models (Arroyo-Currás et al., 2017), it is not surprising that the standard one-compartment model is only (tied for being) the preferred model in one out of the ten datasets (Table 3). This said, however, the standard two-compartment model is only ranked the preferred (or tied for being the preferred) model in half of our ten datasets. This is because two of the time-varying one-compartment models, the exponentially- and reciprocally-varying models, perform quite well. In contrast, the linearly-varying model, which we feel is physiologically naïve, is not the preferred model in any of our datasets, and is outperformed by the standard two-compartment model in nine of ten datasets. Reported parameter estimates in Table 3 return similar results as those seen in Lin et al. (1994), a previous tobramycin study in rats. Standard graphical checks and plots illustrating the estimated time-variance of the elimination proportionality are presented for all models across all animals in the SI.

The reciprocally time-varying single-compartment model matches or outperforms (in terms of BIC) the standard two-compartment model in half of our ten datasets, suggesting that time dependence of the proportionality between drug concentration and drug elimination is an important component of tobramycin pharmacokinetics in this animal model. Both extensive prior literature and straightforward physiological considerations, however, suggest that highly-time-resolved plasma drug measurements such as these should, as noted previously, exhibit two exponential phases: a fairly rapid (but easily seen, given the high time resolution of these datasets) phase that captures the distribution of the drug into the tissues (e.g., solid organs), and a slower phase associated with elimination via the kidneys (Loftsson, 2015). Consistent with this, the standard two-compartment model is generally the preferred model for our rat datasets for which the estimated distribution rates (k_{PD} and k_{DP})

under the standard two-compartment model are larger (Fig. 5 and Table 3). In contrast, the time-varying one-compartment model is generally preferred for the datasets associated with smaller estimated distribution rates.

Tobramycin pharmacokinetics are most often described using two compartment models (Arroyo-Currás et al., 2017; Vieira et al., 2019), in which there is a significant, rapid distribution phase (representing equilibration between the blood and the slowly equilibrating tissues) prior to the slower elimination phase. Because of this, we suspected that datasets for which the standard two-compartment model was preferred over the one-compartment models might be those exhibiting larger distribution phases, as this phase is not captured by our time-varying one-compartment models. To investigate this possibility, we reanalyzed our datasets after masking (excluding) data corresponding to one distribution lifetime (i.e., $1/\alpha$ in Equation 4) of observations, thereby reducing the impact of the (relatively fast) distribution phases. Consistent with our hypothesis, after this masking, the reciprocally time-varying one-compartment model (which was our most competitive time-varying model in the full data) is preferred over or matches the standard one-compartment model in eight of the ten datasets (Table 4). (Note: in one case the nonlinear least squares estimation did not converge – presumably due to some models being too complex to fit based on remaining data after masking. Any models for which estimation did not converge we considered non-preferred.) Further details of masking are presented in the SI.

Prior studies of tobramycin in an analogous rat animal models indicate that the proportionality describing the relationship between plasma drug concentration and the elimination rate can change several-fold over the course of hours (Arroyo-Currás et al., 2017, 2018b). For example, using the standard two-compartment model to fit sequential intravenous, bolus tobramycin injections in individual rats, the elimination proportionalities were seen to fall by 10 to 55% over ~2 h (Arroyo-Currás et al., 2017). Likewise, during the course of the feedback-controlled maintenance of constant plasma tobramycin concentrations, the elimination proportionality was estimated to have increased approximately three-fold over the course of 4 h (Arroyo-Currás et al., 2018b). Fits of the reciprocally time-varying model to our masked datasets (which we believe reduces the contributions of the distribution phase) produce similar magnitude changes in the elimination proportionality. To demonstrate, we compare the estimated elimination proportionalities of our reciprocally time-varying fits at each of their respective masked, start times (i.e., immediately after the masked data ends) to their estimates 1 h later (Fig. 6). For eight of our ten datasets the estimated $k_E(t)$ proportionality decreases (by 19 to 88%) over this time period (FR1, FR3, FR4, MR1, MR2, MR3, MR4, MR8). For one of the remaining two datasets (FR2) the reciprocally varying model estimates that the proportionality increases by 41%, and for the second (MR5) this model does not converge. Presumably these latter observations reflect the fact that, while a time-varying model is arguably a better approximation of the physiology of a rat than assuming its kidney function is constant, the reciprocally-varying model nevertheless fails to capture the time-varying physiology of some individual animals.

The observed inter-animal variability in the time dependence of the elimination proportionality could stem from a number of sources. For example, prior to the start of

injection, different rats may have been under anesthesia for different lengths of time, and we often see the greatest change in the elimination proportionality early after the start of our measurements. Unfortunately, information regarding the duration of anesthesia prior to the start of infusion is not available. Irrespective, however, of the origins of these inter-animal differences, the strength of the reciprocally time-varying model relative to standard models suggests that time-varying kidney function, a hitherto largely ignored physiological effect, can contribute substantially to the pharmacokinetics of tobramycin, and presumably other (e.g., Dauphin-Ducharme et al., 2019), renally cleared drugs. This said, the clinical implications of this pharmacokinetic variability, such as its impact on clinical decisions based on individualize drug dosing, remain to be explored.

The hour-scale, time-varying physiological effects we identify in tobramycin pharmacokinetics are difficult to identify using the low-time-density datasets traditionally employed in pharmacokinetic studies. To illustrate this difficulty, we also "sparsified" our original datasets by selecting ten equally spaced time-points over the observation period. Fitting the five models described previously to these ten data points, we find that, according to BIC, the one-compartment models are preferred (and are indistinguishable from one another) relative to the standard two-compartment model for rat FR1 (Fig. 7; Table 5). All models except the standard one-compartment model, however, contain at least one parameter with approximate 95% confidence interval spanning zero, implying these sparsified (lower time-density) data do not support the use of models more complex than the standard one-compartment model. Applying this same logic to the remaining nine rats (Table SI5) we see a similar pattern: at least three models are indistinguishable for the majority of rats according to the BIC, and many models produce parameter estimates characterized by excessively wide confidence bounds. We observe similar results (by BIC) when considering alternative sampling schemes in which the majority of the ten samples are collected at either the beginning or the end of the observation period (See SI for data and results).

The results described here strongly suggest that the high time-density and good signal-to-noise of these newly available, EAB-derived pharmacokinetic measurements may justify the use of compartment models more complex than those presented here for tobramycin pharmacokinetics. Unfortunately, however, high-dimensional, time-varying ordinary differential equations are notoriously difficult to solve in closed form, with only a handful of special cases having known analytical solutions (Aplevich, 2000). And any extension of the standard two-compartment ordinary differential equation systems to models that include a time-varying elimination proportionality in Equation 3 (that is, k_E being time-dependent) would result in a system that does not have a known analytical solution analogous to Equation 4a. Without such a known solution, the standard nonlinear least squares methods by which we estimated parameters in this paper cannot be applied.

Conclusions

EAB sensors provide an unprecedented route to seconds-resolved pharmacokinetic data. Here we have used statistical methods to explore the ability of the resulting high-density pharmacokinetic datasets to describe with good statistical significance time-varying models that encompass subtle, hour-to-hour changes in the ability of the kidneys to eliminate the

drug. Doing so we have found that time-varying one-compartment models describe the data just as well as, and often better than, the standard two-compartment model. Moreover, when the impact of the initial, rapid distribution phase is reduced by masking the data, the reciprocally time-varying model becomes preferred over the standard one-compartment model for eight of the ten datasets. These results suggest that the inclusion of time-varying elimination can improve the accuracy with which we can model the pharmacokinetics of tobramycin, and presumably other, renally cleared drugs, an observation that matches our intuition that varying kidney function can be a significant contributor to their pharmacokinetics. Looking to the future, extending these same time-varying ideas for the two-compartment model may improve the accuracy of pharmacokinetic modeling still further; while analytical solutions may not exist, numerical approaches may prove a fruitful means to this end. We close by noting that the recent, rapid expansion of the number of drugs for which EAB-derived, seconds-resolved pharmacokinetics are available, suggests that further exploration of such models would be timely.

Supplementary Material

Refer to Web version on PubMed Central for supplementary material.

Funding

This work was funded under NIH grant EB022015 (to KWP and TK).

Data availability statement

Data used to support these findings can be obtained from the corresponding authors upon request.

References

Akaike H (1974). A New Look at the Statistical Model Identification. IEEE Transactions on Automatic Control, 19(6), 716–723. 10.1109/TAC.1974.1100705

Aplevich JD (2000). The Essentials of Linear State-Space Systems. In The Essentials of Linear State-Space Systems. Wiley.

Arroyo-Currás N, Dauphin-Ducharme P, Ortega G, Ploense KL, Kippin TE, & Plaxco KW (2018a). Subsecond-Resolved Molecular Measurements in the Living Body Using Chronoamperometrically Interrogated Aptamer-Based Sensors. ACS Sensors, 3(2), 360–366. 10.1021/acssensors.7b00787 [PubMed: 29124939]

Arroyo-Currás N, Ortega G, Copp DA, Ploense KL, Plaxco ZA, Kippin TE, Hespanha JP, & Plaxco KW (2018b). High-Precision Control of Plasma Drug Levels Using Feedback-Controlled Dosing. ACS Pharmacology & Translational Science, 1(2), 110–118. 10.1021/acsptsci.8b00033 [PubMed: 32219207]

Arroyo-Currás N, Somerson J, Vieira PA, Ploense KL, Kippin TE, & Plaxco KW (2017). Real-time measurement of small molecules directly in awake, ambulatory animals. Proceedings of the National Academy of Sciences, 114(4), 645–650. 10.1073/pnas.1613458114

Chamorro-Garcia A, Gerson J, Flatebo C, Fetter L, Downs AM, Emmons N, Ennis HL, Milosavić N, Yang K, Stojanovic M, Ricci F, Kippin TE, & Plaxco KW (2022). Real-Time, Seconds-Resolved Measurements of Plasma Methotrexate In Situ in the Living Body. ACS Sensors. 10.1021/acssensors.2c01894

Chen JS, Pulugundla N, Wolfson MR, & Shaffer TH (2014). Pharmacokinetics of Gentamicin by Intravenous and Intratracheal Administrations. 2014 IEEE Signal Processing in Medicine and Biology Symposium (SPMB), 1–6. 10.1109/SPMB.2014.7002952

Dauphin-Ducharme P, Yang K, Arroyo-Currás N, Ploense KL, Zhang Y, Gerson J, Kurnik M, Kippin TE, Stojanovic MN, & Plaxco KW (2019). Electrochemical Aptamer-Based Sensors for Improved Therapeutic Drug Monitoring and High-Precision, Feedback-Controlled Drug Delivery. ACS Sensors, 4(10), 2832–2837. 10.1021/acssensors.9b01616 [PubMed: 31556293]

Downs AM, Gerson J, Leung KK, Honeywell KM, Kippin T, & Plaxco KW (2022). Improved Calibration of Electrochemical Aptamer-Based Sensors. Scientific Reports, 12(1), 5535. 10.1038/s41598-022-09070-7 [PubMed: 35365672]

Fabozzi FJ (2014). Appendix E: Model Selection Criterion: AIC and BIC. In Focardi SM, Rachev ST, & Arshanapalli BG, The Basics of Financial Econometrics (pp. 399–403). P. 10.1002/9781118856406.app5

Fontova P, Colom H, Rigo-Bonnin R, van Merendonk LN, Vidal-Alabró A, Montero N, Melilli E, Meneghini M, Manonelles A, Cruzado JM, Torras J, Grinyó JM, Bestard O, & Lloberas N (2021). Influence of the Circadian Timing System on Tacrolimus Pharmacokinetics and Pharmacodynamics After Kidney Transplantation. Frontiers in Pharmacology, 12, 636048. 10.3389/fphar.2021.636048 [PubMed: 33815118]

Gaskin TL, & Duffull SB (1997). Enhanced gentamicin clearance associated with ileostomy fluid loss. Australian and New Zealand Journal of Medicine, 27(2), 196–197. 10.1111/j.1445-5994.1997.tb00948.x [PubMed: 9145193]

Idili A, Arroyo-Currás N, Ploense KL, Csordas AT, Kuwahara M, Kippin TE, & Plaxco KW (2019). Seconds-resolved pharmacokinetic measurements of the chemotherapeutic irinotecan in situ in the living body. Chemical Science, 10(35), 8164–8170. 10.1039/C9SC01495K [PubMed: 31673321]

Kuypers DRJ, Claes K, Evenepoel P, Maes B, Coosemans W, Pirenne J, & Vanrenterghem Y (2004). Time-Related Clinical Determinants of Long-Term Tacrolimus Pharmacokinetics in Combination Therapy with Mycophenolic Acid and Corticosteroids. Clinical Pharmacokinetics, 43(11), 741–762. 10.2165/00003088-200443110-00005 [PubMed: 15301578]

Leung KK, Downs AM, Ortega G, Kurnik M, & Plaxco KW (2021). Elucidating the Mechanisms Underlying the Signal Drift of Electrochemical Aptamer-Based Sensors in Whole Blood. ACS Sensors, 6(9), 3340–3347. 10.1021/acssensors.1c01183 [PubMed: 34491055]

Lin L, Grenier L, Bergeron Y, Simard M, Bergeron MG, Labrecque G, & Beauchamp D (1994). Temporal Changes of Pharmacokinetics, Nephrotoxicity, and Subcellular Distribution of Tobramycin in Rats. Antimicrobial Agents and Chemotherapy, 38(1), 54–60. 10.1128/AAC.38.1.54 [PubMed: 8141580]

Loftsson T (Ed.). (2015). Essential Pharmacokinetics: A Primer for Pharmaceutical Scientists. Academic Press. 10.1016/B978-0-12-801411-0.00009-3

Mao J, Qiu X, Qin W, Xu L, Zhang M, & Zhong M (2021). Factors Affecting Time-Varying Clearance of Cyclosporine in Adult Renal Transplant Recipients: A Population Pharmacokinetic Perspective. Pharmaceutical Research, 38(11), 1873–1887. 10.1007/s11095-021-03114-9 [PubMed: 34750720]

National Research Council (U.S.), Institute for Laboratory Animal Research (U.S.), & National Academies Press (U.S.) (Eds.). (2011). Guide for the Care and Use of Laboratory Animals (8th ed). National Academies Press.

Petitcollin A, Bensalem A, Verdier M-C, Tron C, Lemaitre F, Paintaud G, Bellissant E, & Ternant D (2020). Modelling of the Time-Varying Pharmacokinetics of Therapeutic Monoclonal Antibodies: A Literature Review. Clinical Pharmacokinetics, 59(1), 37–49. 10.1007/s40262-019-00816-7 [PubMed: 31452150]

Reinhard MK, Bekersky I, Sanders TW, Harris BJ, & Hottendorf GH (1994). Effects of Polyaspartic Acid on Pharmacokinetics of Tobramycin in Two Strains of Rat. Antimicrobial Agents and Chemotherapy, 38(1), 79–82. 10.1128/AAC.38.1.79 [PubMed: 8141585]

Schwarz G (1978). Estimating the Dimension of a Model. The Annals of Statistics, 6(2), 461–464. 10.1214/aos/1176344136

Ritchie HA, & Duffull SB (1998). Another case of high gentamicin clearance and volume of distribution in a patient with high output ileostomy. Australian and New Zealand Journal of Medicine, 28(2), 212–213. 10.1111/j.1445-5994.1998.tb02973.x [PubMed: 9612532]

Seber GAF, & Wild CJ (2003). Nonlinear Regression. Wiley-Interscience.

Vieira PA, Shin CB, Arroyo-Currás N, Ortega G, Li W, Keller AA, Plaxco KW, & Kippin TE (2019). Ultra-High-Precision, in-vivo Pharmacokinetic Measurements Highlight the Need for and a Route Toward More Highly Personalized Medicine. Frontiers in Molecular Biosciences, 6, 69. 10.3389/fmolb.2019.00069 [PubMed: 31475156]

Wahlby U, Thomson AH, Milligan PA, & Karlsson MO (2004). Models for time-varying covariates in population pharmacokinetic-pharmacodynamic analysis. British Journal of Clinical Pharmacology, 58(4), 367–377. 10.1111/j.1365-2125.2004.02170.x [PubMed: 15373929]

Wang E, Sandoval RM, Campos SB, & Molitoris BA (2010). Rapid diagnosis and quantification of acute kidney injury using fluorescent ratio-metric determination of glomerular filtration rate in the rat. American Journal of Physiology-Renal Physiology, 299(5), F1048–F1055. 10.1152/ajprenal.00691.2009 [PubMed: 20685826]

Warne DJ, Baker RE, & Simpson MJ (2019). Using Experimental Data and Information Criteria to Guide Model Selection for Reaction–Diffusion Problems in Mathematical Biology. Bulletin of Mathematical Biology, 81(6), 1760–1804. 10.1007/s11538-019-00589-x [PubMed: 30815837]

Wasfi LA (1993). The Effect of Endotoxin on Tobramycin Pharmacokinetics in Young and Aged Rats. Pharmacology, 47(4), 261–267. 10.1159/000139106 [PubMed: 8234415]

Wilkins JJ, Brockhaus B, Dai H, Vugmeyster Y, White JT, Brar S, Bello CL, Neuteboom B, Wade JR, Girard P, & Khandelwal A (2019). Time-Varying Clearance and Impact of Disease State on the Pharmacokinetics of Avelumab in Merkel Cell Carcinoma and Urothelial Carcinoma. CPT: Pharmacometrics & Systems Pharmacology, 8(6), 415–427. 10.1002/psp4.12406 [PubMed: 30980481]

Xiao Y, Lubin AA, Heeger AJ, & Plaxco KW (2005). Label-Free Electronic Detection of Thrombin in Blood Serum by Using an Aptamer-Based Sensor. Angewandte Chemie International Edition, 44(34), 5456–5459. 10.1002/anie.200500989 [PubMed: 16044476]

What is already known about this subject:

- While the pharmacokinetics of many drugs are known to vary over weeks to months timescales, until recently the possibility of hours-scale pharmacokinetic variability has not been experimentally addressable.
- New *in-vivo* molecular measurement approaches, however support seconds-resolved pharmacokinetic characterization, providing a new opportunity to detect far more rapid changes in pharmacokinetics.
- The first studies using these approaches, which characterized the clearance of successive bolus intravenous injections, suggested that changing kidney function can measurably alter the elimination kinetics of renally cleared drugs over just hours.

What this study adds:

- Using time-dense (equally spaced, seconds-resolved) *in-vivo* measurements of plasma tobramycin concentrations we have identified statistically significant, hour-scale variations in the proportionality between elimination rate and plasma drug levels in the majority of animals studied.

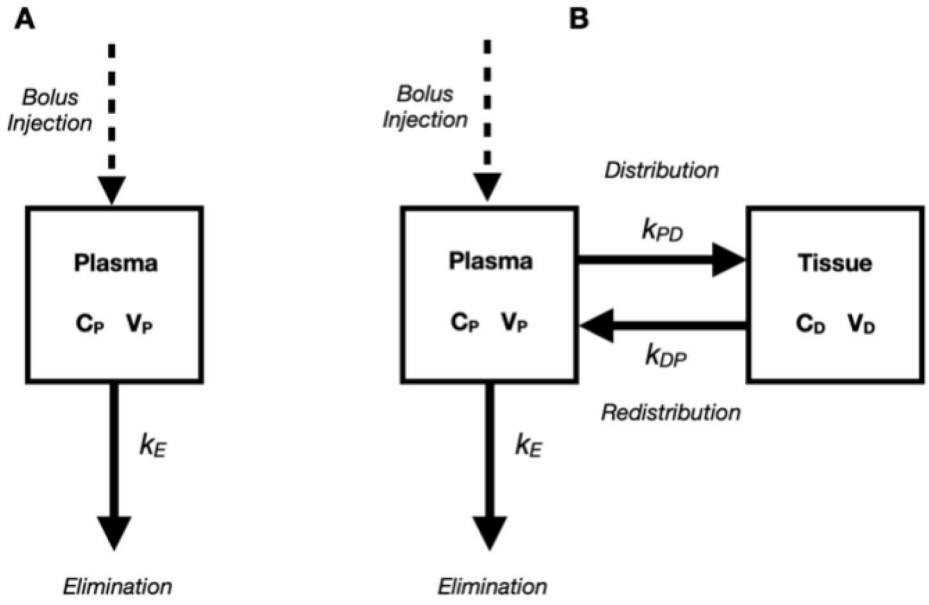

Figure 1.

Shown are schematics of traditional one- and two-compartment pharmacokinetic models with intravenous bolus drug delivery. (A) The one-compartment model is the simplest approximation of the drug elimination process after an intravenous bolus delivery, treating the body as a single entity (compartment). (B) The two-compartment model increases the complexity, by adding a second compartment (the tissue compartment) for the drug to distribute through. C_P and C_D represent the plasma and tissue concentrations respectively (subsequently written $C_P(t)$ and $C_D(t)$ to indicate time t). V_P and V_D represent the corresponding theoretical volumes of distribution. k_E represents the elimination rate of drug leaving the compartmental system, while k_{PD} and k_{DP} represent the drug exchange rates between the two compartments.

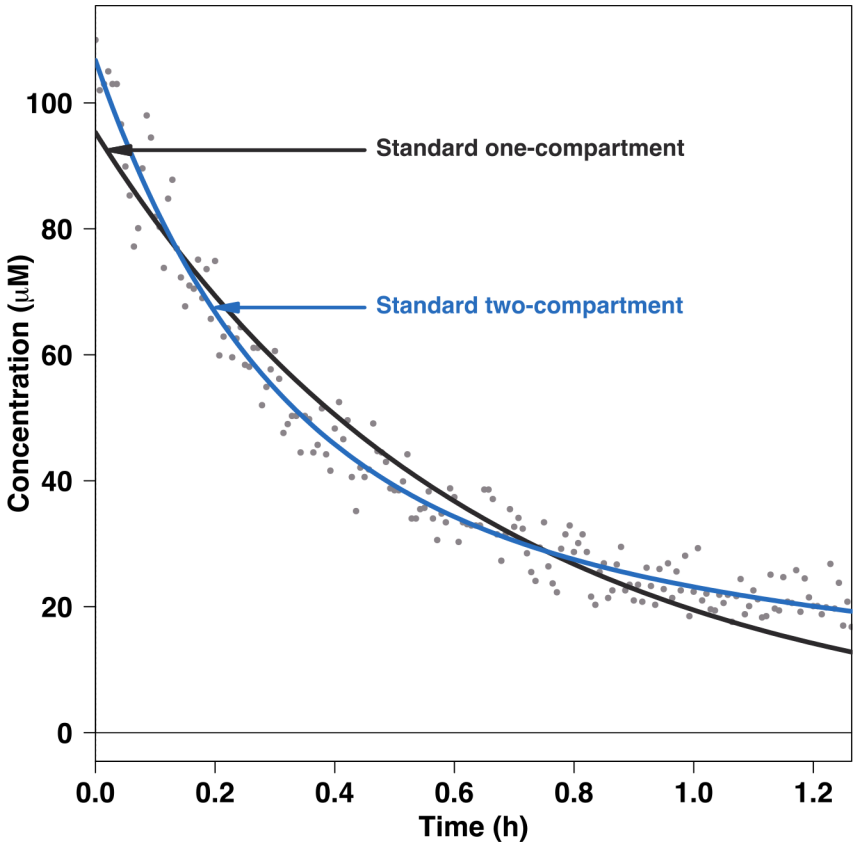

Figure 2.

As seen by deviations at the extrema, the nonlinear least squares regression fit for the standard one-compartment model (Equation 2) fails to adequately capture the concentration-time profile for Female Rat 1 (FR1). In contrast, the standard two-compartment model fit captures both the rapid decrease during the initial distribution phase and the slower decrease during elimination phase seen towards the end of the experiment (Equation 4a). Data and fits for the remaining rats are presented in Figure 5.

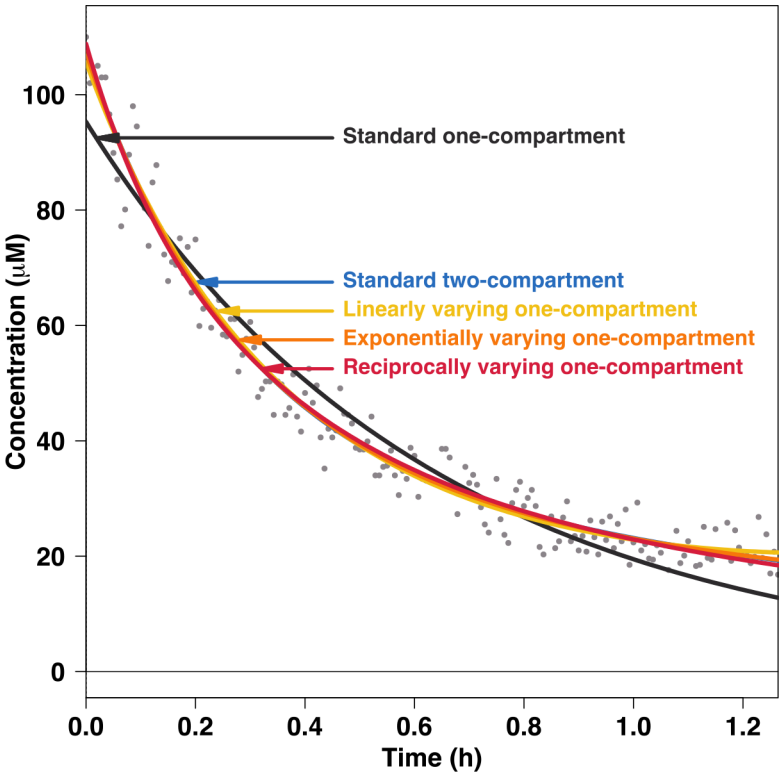

Figure 3.

When applied to the pharmacokinetics of tobramycin in Female Rat 1, all three time-varying one-compartment models (Table 1) outperform both the standard one- and two-compartment models when judged using BIC (shown in Table 2). Indeed, as shown, the fits of all three time-varying models are visually almost indistinguishable from that of the standard two-compartment model, with only subtle differences being seen at the tail ends of the fits.

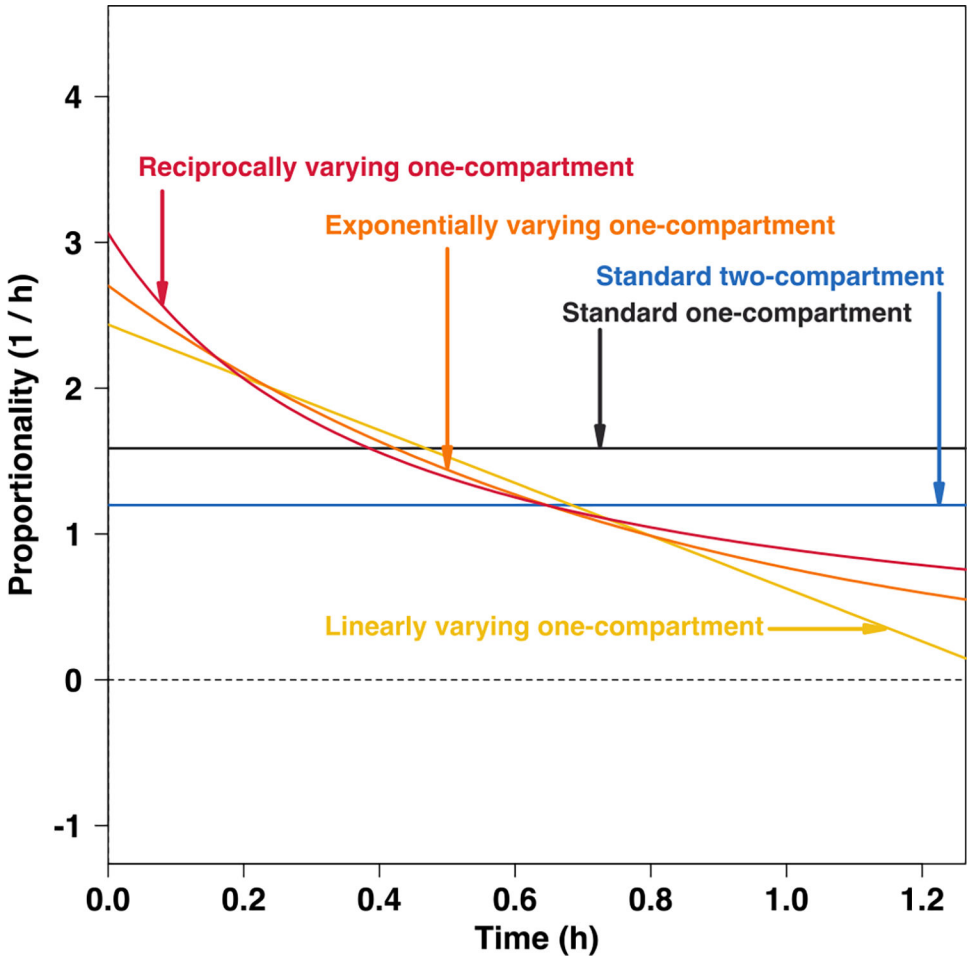

Figure 4.

When applied to the FR1 dataset, the time-varying one-compartment models produce monotonically decreasing elimination proportionality estimates. This matches physiological intuition, which is that kidney function, and thus the renal elimination of this drug, falls with time due to the dehydration and loss of blood pressure that occurs for animals under anesthesia without an intravenous drip.

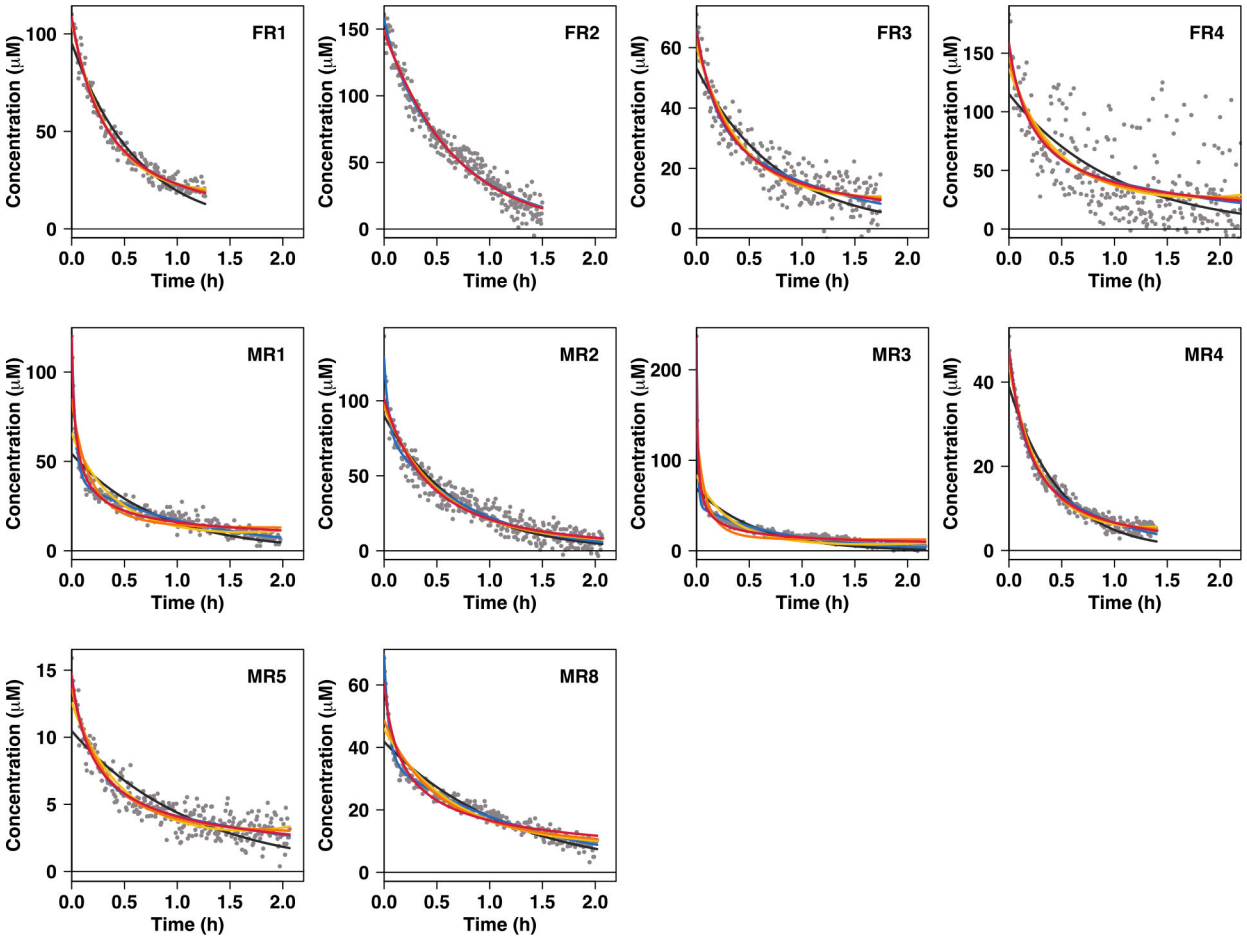

Figure 5.

The fits of the time-varying one-compartment models are almost indistinguishable from those of the standard two-compartment model. To illustrate this, here we present the observed concentrations (dots) versus time profiles with fitted pharmacokinetic profiles for all five model we have considered (solid curves). For the majority of our datasets, the time-varying one-compartment model fits (red, orange, yellow curves) visually are almost indistinguishable from those of the standard two-compartment model (blue curve). The constant-elimination rate one-compartment model (black curve) is the preferred model for only one dataset (FR2). The high variability seen in the FR4 observations is presumably due to a noisy sensor; the signal-to-noise of these handmade devices sometimes varies due to placement (i.e., nearer or farther from the heart), residual animal motion, poor connections, or variations in sensor size.

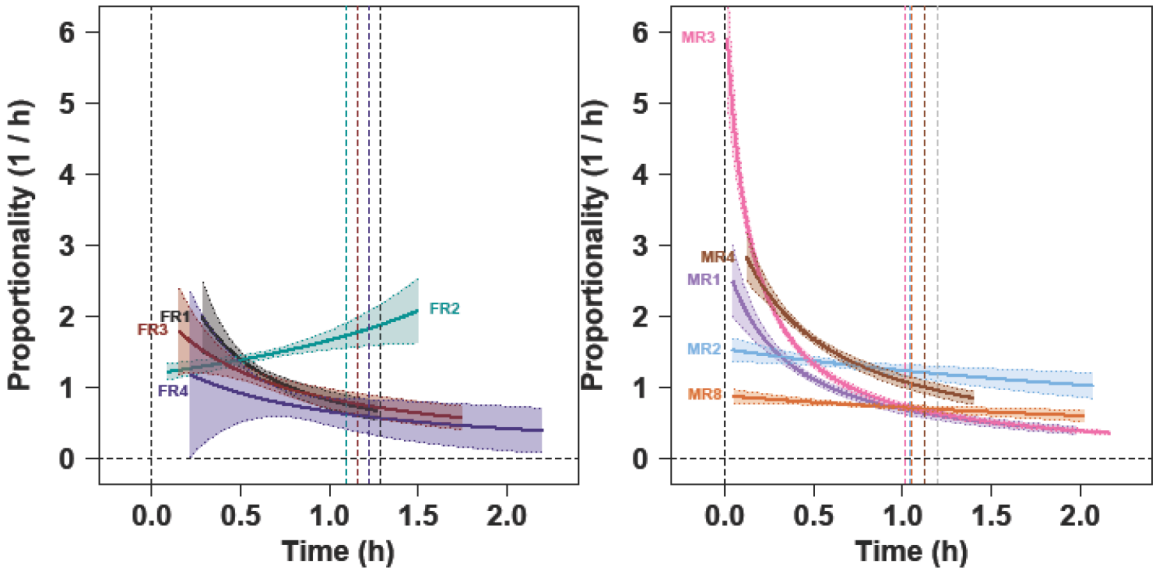

Figure 6.

Estimated proportionalities $k_E(t)$ (solid curves) from fitting reciprocally time-varying one-compartment models to our masked data (in which data corresponding to one estimated distribution lifetime has been removed from the beginning of the data run), suggest significant intra- and inter-animal variability in kidney function. The left plot illustrates female rats, and the right male rats. Approximate 95% pointwise confidence bands are shown for each animal's respective observation period (dotted curves, shaded area), excluding MR5 due to non-convergence.

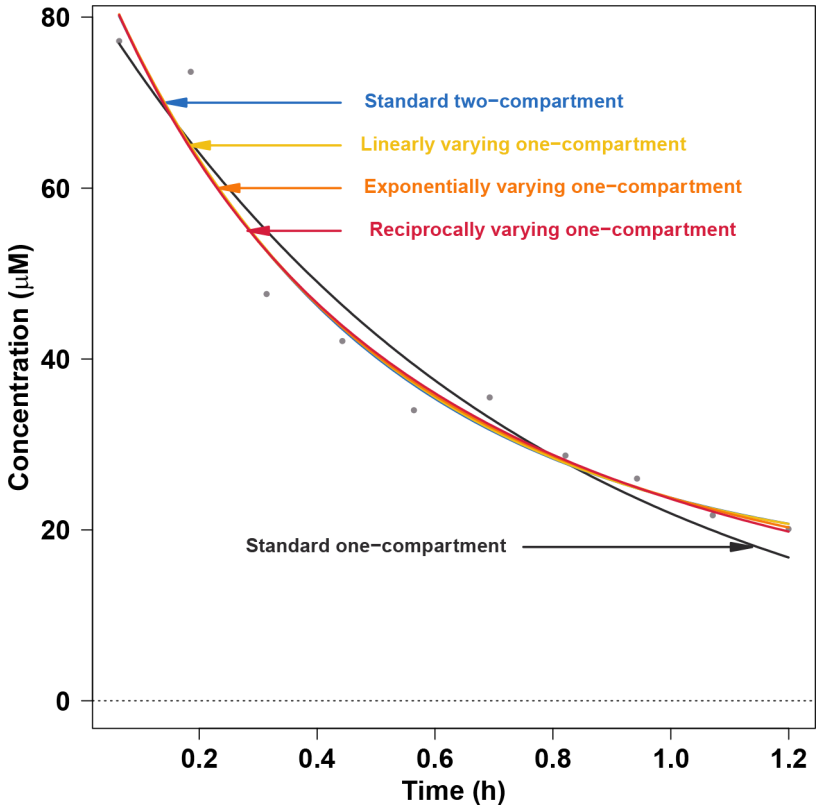

Figure 7.

The sparse datasets traditionally employed in pharmacokinetic studies are insufficient to capture subtle, time-varying physiological effects of the type described here. To illustrate this, we selected ten equally spaced time-points from FR1 data (displayed in Fig. 3), and fitted our five models to the resulting, sparser dataset. Although all of our one-compartment models describe this sparse dataset equally well (according to BIC), all of the models except the standard one-compartment model contain at least one parameter with approximate 95% confidence interval encompassing zero, implying these sparser data do not support the use of models more complex than the standard one-compartment model. In the SI we present similar analyses employing unequally spaced sparse datasets (Fig. SI2–SI3).

Table 1:

The time-varying one-compartment models explored here

Model	Elimination Proportionality	ODE Solution
Linear	$k_E(t) = b_E \cdot t + k_{E0}$	$C_P(t) = \frac{D_0}{V_P} \cdot \exp\left\{-\left(\frac{b_E}{2} \cdot t + k_{E0}\right)t\right\}$
Exponential	$k_E(t) = k_{E0}e^{-b_E \cdot t}$	$C_P(t) = \frac{D_0}{V_P} \cdot \exp\left\{\frac{k_{E0}}{b_E}\left(e^{-b_E \cdot t} - 1\right)\right\}$
Reciprocal	$k_E(t) = \frac{k_{E0}}{(b_E \cdot t + 1)}$	$C_P(t) = \frac{D_0}{V_P} \cdot \exp\left\{-\frac{k_{E0}}{b_E}\ln(b_E \cdot t + 1)\right\}$

Table 2:

BIC, AIC, RMSE, parameter estimates and 95% approximate confidence bounds for Female Rat 1

Parameters and Model Measures	One-compartment				Two-compartment	No. Obs.	Dur. (h)
	Standard	Linear	Exponential	Reciprocal	Standard		
V_P (mL)	106 ± 3	95 ± 2	94 ± 2	93 ± 3	94 ± 3	178	1.26
k_E (h^{-1})	1.59 ± 0.07	-	-	-	1.2 ± 0.5		
k_{E0} (h^{-1})	-	2.4 ± 0.1	2.7 ± 0.2	3.1 ± 0.3	-		
b_E (h^{-1} or h^{-2})	-	−1.8 ± 0.2	1.2 ± 0.2	2.4 ± 0.6	-		
k_{PD} (h^{-1})	-	-	-	-	1.4 ± 0.3		
k_{DP} (h^{-1})	-	-	-	-	1.5 ± 1.2		
BIC [a]	**1133.6**	**1007.7**	**1005.5**	**1008.4**	**1011.4**		
AIC [a]	**1124.1**	**995.0**	**992.7**	**995.6**	**995.5**		
RMSE[a]**(μM)**	**5.59**	**3.87**	**3.85**	**3.88**	**3.85**		

[a]For definitions of BIC (Bayesian Information Criterion), AIC (Akaike Information Criterion), and RMSE (root-mean-squared error), see SI.

The preferred model as selected by the BIC is shaded in grey.

Table 3:

BIC. AIC. RMSE. parameter estimates and approximate 95% confidence bounds for all models/all animals

Rat	Parameters and Model Measures	One-compartment				Two-compartment	No. Obs.	Dur. (h)
		Standard	Linear	Exponential	Reciprocal	Standard		
FR1	V_P (mL)	106 ± 3	95 ± 2	94 ± 2	93 ± 3	95 ± 3	178	1.26
	k_E (h^{-1})	1.59 ± 0.07	-	-	-	1.2 ± 0.5		
	k_{E0} (h^{-1})	-	2.4 ± 0.1	2.7 ± 0.2	3.1 ± 0.3	-		
	b_E (h^{-1} or h^{-2})	-	−1.8 ± 0.2	1.3 ± 0.2	2.4 ± 0.6	-		
	k_{PD} (h^{-1})	-	-	-	-	1.4 ± 0.3		
	k_{DP} (h^{-1})	-	-	-	-	1.5 ± 1.2		
	BIC [a]	**1133.6**	**1007.7**	**1005.5**	**1008.4**	**1011.4**		
	AIC [a]	**1124.1**	**995.0**	**992.7**	**995.6**	**995.5**		
	RMSE[a](μM)	**5.59**	**3.87**	**3.85**	**3.88**	**3.85**		
FR2	V_P (mL)	67.9 ± 1.3	68 ± 2	68 ± 2	68 ± 2	63 ± 3	293	1.5
	k_E (h^{-1})	1.51 ± 0.05	-	-	-	1.57 ± 0.09		
	k_{E0} (h^{-1})	-	1.5 ± 0.1	1.5 ± 0.1	1.5 ± 0.1	-		
	b_E (h^{-1} or h^{-2})	-	−0.01 ± 0.23	0.0 ± 0.2	0.01 ± 0.16	-		
	k_{PD} (h^{-1})	-	-	-	-	0.9 ± 1.3		
	k_{DP} (h^{-1})	-	-	-	-	10.4 ± 12		
	BIC [a]	**2071.4**	**2077.1**	**2077.1**	**2077.1**	**2070.6**		
	AIC [a]	**2060.3**	**2062.3**	**2062.3**	**2062.3**	**2052.2**		
	RMSE[a](μM)	**8.06**	**8.06**	**8.06**	**8.06**	**7.89**		
FR3	V_P (mL)	191 ± 8	168 ± 8	162 ± 8	154 ± 10	153 ± 11	245	1.74
	k_E (h^{-1})	1.29 ± 0.09	-	-	-	1.4 ± 0.16		
	k_{E0} (h^{-1})	-	2.1 ± 0.2	2.5 ± 0.4	3.4 ± 0.8	-		
	b_E (h^{-1} or h^{-2})	-	−1.3 ± 0.3	1.2 ± 0.3	3.5 ± 1.5	-		
	k_{PD} (h^{-1})	-	-	-	-	2.1 ± 0.9		
	k_{DP} (h^{-1})	-	-	-	-	3.9 ± 2.0		
	BIC [a]	**1574.6**	**1519.1**	**1511.6**	**1506.0**	**1512.7**		
	AIC [a]	**1564.1**	**1505.1**	**1497.6**	**1492.0**	**1495.2**		
	RMSE[a](μM)	**5.82**	**5.14**	**5.06**	**5**	**5.01**		
FR4	V_P (mL)	88 ± 8	75 ± 8	70 ± 8	64 ± 10	67 ± 9	291	2.2
	k_E (h^{-1})	1.0 ± 0.1	-	-	-	1.0 ± 0.4		
	k_{E0} (h^{-1})	-	1.8 ± 0.4	2.4 ± 0.8	4.2 ± 2.6	-		
	b_E (h^{-1} or h^{-2})	-	−1.0 ± 0.4	1.4 ± 0.6	5.9 ± 5.5	-		

Rat	Parameters and Model Measures	One-compartment				Two-compartment	No. Obs.	Dur. (h)
		Standard	Linear	Exponential	Reciprocal	Standard		
	k_{PD} (h^{-1})	-	-	-	-	1.9 ± 1.3		
	k_{DP} (h^{-1})	-	-	-	-	2.3 ± 2.3		
	BIC [a]	**2801.3**	**2783.9**	**2781.1**	**2779.3**	**2787.0**		
	AIC [a]	**2790.3**	**2769.2**	**2766.4**	**2764.6**	**2768.6**		
	RMSE[a]**(μM)**	**28.94**	**27.81**	**27.68**	**27.59**	**27.69**		
MR1	V_P (mL)	280 ± 15	232 ± 13	179 ± 10	126 ± 7	129 ± 6	268	1.98
	k_E (h^{-1})	1.2 ± 0.1	-	-	-	2.4 ± 0.1		
	k_{E0} (h^{-1})	-	2.3 ± 0.2	5.3 ± 0.6	28 ± 6	-		
	b_E (h^{-1} or h^{-2})	-	−1.4 ± 0.3	2.8 ± 0.4	57 ± 14	-		
	k_{PD} (h^{-1})	-	-	-	-	16 ± 2		
	k_{DP} (h^{-1})	-	-	-	-	9.5 ± 1.0		
	BIC [a]	**1868.3**	**1800.4**	**1715.2**	**1491.2**	**1379.2**		
	AIC [a]	**1857.5**	**1786.0**	**1700.8**	**1476.8**	**1361.3**		
	RMSE[a]**(μM)**	**7.66**	**6.67**	**5.69**	**3.75**	**3.01**		
MR2	V_P (mL)	131 ± 4	123 ± 4	121 ± 4	116 ± 4	92 ± 6	373	2.07
	k_E (h^{-1})	1.44 ± 0.06	-	-	-	2.0 ± 0.1		
	k_{E0} (h^{-1})	-	1.8 ± 0.1	1.99 ± 0.18	2.4 ± 0.3	-		
	b_E (h^{-1} or h^{-2})	-	−0.6 ± 0.2	0.5 ± 0.2	1.2 ± 0.4	-		
	k_{PD} (h^{-1})	-	-	-	-	8 ± 3		
	k_{DP} (h^{-1})	-	-	-	-	16 ± 4		
	BIC [a]	**2534.6**	**2508.0**	**2500.0**	**2487.3**	**2391.4**		
	AIC [a]	**2522.8**	**2492.3**	**2484.3**	**2471.6**	**2371.8**		
	RMSE[a] (m.M)	**7.06**	**6.76**	**6.69**	**6.58**	**5.74**		
MR3	V_P (mL)	165 ± 12	136 ± 10	84 ± 6	48.3 ± 1.8	50 ± 2	326	2.17
	k_E (h^{-1})	1.8 ± 0.2	-	-	-	5.3 ± 0.2		
	k_{E0} (h^{-1})	-	3.0 ± 0.3	11± 2	124 ± 18	-		
	b_E(h^{-1} or h^{-2})	-	−1.8 ± 0.4	4.7 ± 0.6	247 ± 42	-		
	k_{PD} (h^{-1})	-	-	-	-	60 ± 5		
	k_{DP} (h^{-1})	-	-	-	-	19± 1		
	BIC [a]	**2552.3**	**2501.3**	**2405.6**	**1922.8**	**1779.7**		
	AIC [a]	**2541.0**	**2486.2**	**2390.4**	**1907.6**	**1760.8**		
	RMSE[a]**(μM)**	**11.81**	**10.83**	**9.35**	**4.46**	**3.55**		
MR4	V_P (mL)	383 ± 10	339 ± 6	327 ± 7	314 ± 7	312 ± 7	273	1.4

Rat	Parameters and Model Measures	One-compartment				Two-compartment	No. Obs.	Dur. (h)
		Standard	Linear	Exponential	Reciprocal	Standard		
	k_E (h^{-1})	2.07 ± 0.08	-	-	-	2.25 ± 0.09		
	k_{E0} (h^{-1})	-	3.2 ± 0.1	3.8 ± 0.2	4.8 ± 0.4	-		
	b_E (h^{-1} or h^{-2})	-	−2.5 ± 0.2	1.51 ± 0.13	3.8 ± 0.6	-		
	k_{PD} (h^{-1})	-	-	-	-	2.6 ± 0.4		
	k_{DP} (h^{-1})	-	-	-	-	4.9 ± 0.9		
	BIC [a]	**1281.2**	**1038.7**	**999.8**	**967.3**	**980.0**		
	AIC [a]	**1270.4**	**1024.3**	**985.4**	**952.9**	**962.0**		
	RMSE[a](μM)	**2.45**	**1.56**	**1.45**	**1.37**	**1.38**		
MR5	V_P (mL)	1531±59	1276 ± 45	1180 ± 48	1092 ± 60	1147±56	290	2.06
	k_E (h^{-1})	0.87 ± 0.06	-	-	-	0.8 ± 0.1		
	k_{E0} (h^{-1})	-	1.7 ± 0.1	2.5 ± 0.3	4.4 ± 1.0	-		
	b_E (h^{-1} or h^{-2})	-	−1.1 ± 0.1	1.6 ± 0.2	7.4 ± 2.5	-		
	k_{PD} (h^{-1})	-	-	-	-	2.0 ± 0.4		
	k_{DP} (h^{-1})	-	-	-	-	2.3 ± 0.7		
	BIC [a]	**952.5**	**802.3**	**769.9**	**758.2**	**770.6**		
	AIC [a]	**941.5**	**787.6**	**755.2**	**743.6**	**752.3**		
	RMSE[a](μM)	**1.21**	**0.93**	**0.88**	**0.86**	**0.87**		
MR8	V_P (mL)	402 ± 12	366 ± 12	346 ± 12	278 ± 13	242 ± 8	283	2.02
	k_E (h^{-1})	0.85 ± 0.04	-	-	-	1.31 ± 0.05		
	k_{E0} (h^{-1})	-	1.3 ± 0.1	1.7 ± 0.2	5.4 ± 1.1	-		
	b_E (h^{-1} *or* h^{-2})	-	−0.5 ± 0.1	0.9 ± 0.2	10 ± 3	-		
	k_{PD} (h^{-1})	-	-	-	-	9.6 ± 1.3		
	k_{DP} (h^{-1})	-	-	-	-	11.5 ± 1.2		
	BIC [a]	**1547.0**	**1501.9**	**1477.3**	**1393.1**	**1089.1**		
	AIC [a]	**1536.0**	**1487.4**	**1462.7**	**1378.5**	**1070.8**		
	RMSE[a](μM)	**3.61**	**3.3**	**3.16**	**2.72**	**1.58**		
Times model is best or matches best		1/10	0/10	2/10	4/10	5/10		
Times model betters or matches two-compartment model		1/10	1/10	4/10	5/10			

[a]For definitions of BIC (Bayesian Information Criterion), AIC (Akaike Information Criterion), and RMSE (root-mean- squared error), see SI. The preferred model or models for each rat (by the BIC) are shaded grey.

Table 4:

BIC, AIC, RMSE, parameter estimates and approximate 95% confidence bounds, based on all observations after removing estimated distribution phase of each rat

Rat	Parameters and Model Measures	One-compartment		No. Obs.	Dur. (h)
		Standard	Reciprocal		
FR1	V_P (mL)	139 ± 7	78 ± 42	138	0.98
	k_E (h^{-1})	1.16 ± 0.07	-		
	k_{E0} (h^{-1})	-	4.5 ± 4.9		
	b_E (h^{-1} or h^{-2})	-	4.5 ± 6.7		
	k_{PD} (h^{-1})	-	-		
	k_{DP} (h^{-1})	-	-		
	BIC [a]	**762.4**	**743.8**		
	AIC [a]	**753.6**	**732.1**		
	RMSE[a]**(μM)**	**3.6**	**3.3**		
FR2	V_p (mL)	70 ± 2	74 ± 3	275	1.41
	k_E (h^{-1})	1.46 ± 0.05	-		
	k_{E0} (h^{-1})	-	1.2 ± 0.1		
	b_E (h^{-1} or h^{-2})	-	−0.3 ± 0.1		
	k_{PD} (h^{-1})	-	-		
	k_{DP} (h^{-1})	-	-		
	BIC [a]	**1926.6**	**1921.9**		
	AIC [a]	**1915.8**	**1907.5**		
	RMSE[a]**(μM)**	**7.8**	**7.7**		
FR3	V_P (mL)	229 ± 14	178 ± 37	223	1.59
	k_E (h^{-1})	1.0 ± 0.1	-		
	k_{E0} (h^{-1})	-	2.2 ± 1.3		
	b_E (h^{-1} or h^{-2})	-	1.7 ± 1.8		
	k_{PD} (h^{-1})	-	-		
	k_{DP} (h^{-1})	-	-		
	BIC [a]	**1377.2**	**1368.6**		
	AIC [a]	**1367.0**	**1355.0**		
	RMSE[a]**(μM)**	**5.1**	**5.0**		
FR4	V_P (mL)	118 ± 18	94 ± 52	262	1.98
	k_E (h^{-1})	0.7 ± 0.2	-		
	k_{E0} (h^{-1})	-	1.5 ± 2.5		

Rat	Parameters and Model Measures	One-compartment		No. Obs.	Dur. (h)
		Standard	Reciprocal		
	b_E (h^{-1} or h^{-2})	-	1.3 ± 4.2		
	k_{PD} (h^{-1})	-	-		
	k_{DP} (h^{-1})	-	-		
	BIC [a]	**2515.5**	**2518.6**		
	AIC [a]	**2504.8**	**2504.3**		
	RMSE[a]**(μM)**	**28.5**	**28.4**		
MR1	V_P (mL)	344 ± 12	263 ± 19	262	1.93
	k_E (h^{-1})	0.97 ± 0.05	-		
	k_{E0} (h^{-1})	-	2.8 ± 0.7		
	b_E (h^{-1} or h^{-2})	-	3.1 ± 1.3		
	k_{PD} (h^{-1})	-	-		
	k_{DP} (h^{-1})	-	-		
	BIC [a]	**1459.6**	**1403.7**		
	AIC [a]	**1448.9**	**1389.4**		
	RMSE[a]**(μM)**	**3.8**	**3.4**		
MR2	V_P (mL)	142 ± 4	136 ± 5	365	2.02
	k_E (h^{-1})	1.33 ± 0.05	-		
	k_{E0} (h^{-1})	-	1.5 ± 0.2		
	b_E (h^{-1} or h^{-2})	-	0.2 ± 0.2		
	k_{PD} (h^{-1})	-	-		
	k_{DP} (h^{-1})	-	-		
	BIC [a]	**2340.4**	**2340.3**		
	AIC [a]	**2328.7**	**2324.7**		
	RMSE[a]**(μM)**	**5.8**	**5.8**		
MR3	V_P (mL)	205 ± 7	132 ± 7	324	2.15
	k_E (h^{-1})	1.35 ± 0.07	-		
	k_{E0} (h^{-1})	-	6.5 ± 1.1		
	b_E (h^{-1} or h^{-2})	-	7.8 ± 1.9		
	k_{PD} (h^{-1})	-	-		
	k_{DP} (h^{-1})	-	-		
	BIC [a]	**1963.6**	**1732.8**		
	AIC [a]	**1952.3**	**1717.7**		
	RMSE[a]**(μM)**	**4.9**	**3.4**		

Rat	Parameters and Model Measures	One-compartment		No. Obs.	Dur. (h)
		Standard	Reciprocal		
MR4	V_P (mL)	474 ± 14	351 ± 31	249	1.27
	k_E (h^{-1})	1.65 ± 0.06	-		
	k_{E0} (h^{-1})	-	3.6 ± 0.7		
	b_E (h^{-1} or h^{-2})	-	2.3 ± 0.9		
	k_{PD} (h^{-1})	-	-		
	k_{DP} (h^{-1})	-	-		
	BIC [a]	**961.6**	**873.2**		
	AIC [a]	**951.0**	**859.1**		
	RMSE[a]**(μM)**	**1.6**	**1.3**		
MR5	V_P (mL)	1948±98	*DNC* [b]	260	1.85
	k_E (h^{-1})	0.63 ± 0.05			
	k_{E0} (h^{-1})	-			
	b_E (h^{-1} or h^{-2})	-			
	k_{PD} (h^{-1})	-			
	k_{DP} (h^{-1})	-			
	BIC [a]	**718.9**			
	AIC [a]	**708.3**			
	RMSE[a]**(μM)**	**0.9**			
MR8	V_P (mL)	444 ± 8	429 ± 12	276	1.97
	k_E (h^{-1})	0.75± 0.02	-		
	k_{E0} (h^{-1})	-	0.9 ± 0.1		
	b_E (h^{-1} or h^{-2})	-	0.2 ± 0.2		
	k_{PD} (h^{-1})	-	-		
	k_{DP} (h^{-1})	-	-		
	BIC [a]	**1161.3**	**1159.9**		
	AIC [a]	**1150.4**	**1145.4**		
	RMSE[a]**(μM)**	**1.9**	**1.9**		
Times model is best or matches best[c]		3/10	8/10		

[a] For definitions of BIC (Bayesian Information Criterion), AIC (Akaike Information Criterion), and RMSE (root-mean-squared error), see SI. The preferred model as selected by the BIC is shaded in grey.

[b] DNC stands for “did not converge.” This occurs when the convergence criteria is not met within the set iteration limit. For more detail, see the SI.

[c] We treat models where estimation did not converge as non-preferred in the model selection process.

Table 5:

BIC, AIC, RMSE, parameter estimates and approximate 95% confidence bounds for Female Rat 1 when the dataset is reduced to ten equally spaced data points

Parameters and Model Measures	One-compartment				Two-compartment	No. Obs.	Dur. (h)
	Standard	Linear	Exponential	Reciprocal	Standard		
V_P (mL)	120 ± 13	112 ± 14	111 ± 16	111 ± 18	112 ± 20	10	1.14
k_E (h^{-1})	1.3 ± 0.2	-	-	-	1 ± 17		
k_{E0} (h^{-1})	-	1.9 ± 0.7	2.0 ± 1.0	2.1 ± 1.4	-		
b_E (h^{-1} or h^{-2})	-	−1.1 ± 1.3	0.8 ± 1.1	1.2 ± 2.5	-		
k_{PD} (h^{-1})	-	-	-	-	1 ± 15		
k_{DP} (h^{-1})	-	-	-	-	1 ± 11		
BIC [a]	**65.0**	**64.0**	**64.1**	**64.3**	**66.2**		
AIC [a]	**64.1**	**62.8**	**62.9**	**63.1**	**64.7**		
RMSE[a]**(μM)**	**4.4**	**3.8**	**3.8**	**3.8**	**3.7**		

[a]For definitions of BIC (Bayesian Information Criterion), AIC (Akaike Information Criterion), and RMSE (root-mean-squared error), see SI. The preferred models for this rat (by the BIC) are shaded grey.